Journal of the Korean Nuclear Society
Volume 35, Number 6, pp.515~522, December, 2003

Effect of LiOT on the Tritium Inventory of Li_2O Fusion Blanket Breeder Material

S. Cho
Korea Basic Science Institute
52 Yeoeun-dong, Yusung-gu, Daejeon, 305-333, Korea
M.A. Abdou
University of California
California, Los Angeles, USA
sycho@kbsi.re.kr

Abstract

(Received May 6, 2003)

Tritium behavior in the solid breeder blanket is one of the key factors in determining tritium self-sufficiency, as well as safety, of fusion reactors. Recently, a model has been developed to describe the tritium behavior in solid breeder material, which can predict the tritium release and inventory in the blanket. However, the model has limitation to account for tritium solubility effects, mainly existing as LiOT, especially inside the Li_2O solid breeder. In order to improve the capability of predicting the LiOT precipitation in Li_2O solid breeder, a new logic is developed and integrated in the existing tritium release and inventory calculation code. With the logic developed in this work, the code can have capabilities to analyze tritium release and inventories in Li_2O under steady and transient conditions. It can be found that tritium inventory as LiOT is an important mechanism under pulsed operation, and the amount of inventory becomes higher as the tritium generation rate increases and the temperature decreases. Also, the temperature limits for the generation of LiOT precipitation are determined. Therefore the developed logic helps understand the tritium transport mechanism in Li_2O solid breeder.

Key Words : fusion blanket, solid breeder, tritium, LiOT, Li_2O, solubility

1. Introduction

Even though Li_2O-based solid breeder blankets were not considered for ITER [1], lithium oxide has been suggested as a suitable breeding blanket material for a fusion reactor. Tritium release from solid breeder materials has been investigated extensively, and several factors, namely dissolution, diffusion and surface reactions are recognized to participate in the tritium release process [2-5].

The tritium transport and inventory in Li_2O solid breeder of the fusion blanket are affected by the oxygen bearing molecules in the purge gas as well as the solubility of tritium in Li_2O as LiOT. The capability of predicting the LiOT precipitation and the effect on tritium inventory were tested using the MISTRAL code [6,7]. However, the recent

tritium release and inventory analyses in Li_2O solid breeder under steady state and pulsed operating conditions show significant differences between the code predictions and thermodynamic correlations.

MISTRAL code has been developed at UCLA to predict the tritium release and inventory in solid breeder materials in transient as well as steady state conditions. It is based on a model that includes several transport mechanisms, such as diffusion through the grain and grain boundary, surface adsorption and desorption, and diffusion along the interconnected porosity. However, LiOT formation in the ceramic is not included in the code, which can play a key role in determining the tritium inventory in the presence of moisture, especially in the case of Li_2O.

In this study, a logic for predicting LiOT formation and decomposition in Li_2O solid breeder is developed and integrated in the MISTRAL code based on the available thermodynamics and kinetics data for the formation and decomposition of LiOH(T) and the solubility of LiOT in Li_2O. The logic is based on comparison between the local tritium concentration and the LiOT solubility limit at the breeder temperature. With this logic, the code is used to analyze tritium release and inventories in Li_2O under steady and transient conditions. The transient temperature scenario includes both the breeder temperature varied over a wide range from 600℃ to 100℃ and several tritium generation rates in the range of 1×10^{18} to 1×10^{21} atoms/m^3-s. Based on the transient scenario the temperature limits for formation and decomposition of LiOT and the temperature regimes, over which each of the three forms of tritium inventory (grain, surface and precipitation) is dominant, are determined as a function of tritium generation rate.

2. Available Thermodynamics and Kinetics Data

2.1. Solubility Limit of LiOT in Li_2O

While operating the Li_2O solid breeder at high temperatures, the formation of the LiOT is diminished. And its solubility limit in Li_2O increases with increase in temperature and becomes the dominant contributor to the tritium release and inventory. The solubility limit of LiOH in Li_2O has been reported in [8] as:

$$x_{LiOH} = 17.3 \times [9.872 \times 10^{-6} \times P_{H2O}]^{(0.495+13\,4/T)} \times \exp(-8607/T) \quad (1)$$

Where x_{LiOH} is the mole fraction of LiOH and P_{H2O} [Pa] is the partial pressure of water in atmosphere. The water partial pressure over the two-phase Li_2O-LiOH system has been reported in [9-11] and summarized in Table 1. Then the solubility limit is obtained by substituting the partial pressure of water into the solubility of LiOT(H) in Li_2O given by Eq. (1) and the results are expressed in Table 1 and shown graphically in Fig. 1. As shown in the figure, the solubility limit monotonously

Table. 1. Water Partial Pressure, Solubility, and Kinetics of LiOT in Li_2O Solid Breeder

Temperature Range T[K]	Water Partial Pressure P_{H2O}[Pa]	Solubility Limit x_{LiOT}[wppm]Formation	Rate Constant for Formation $k_f[s^{-1}]$
T < 621	$1.498 \times 10^{11} \times \exp(-15090/T)$	$1.568 \times 10^{10} \times \exp(-15890/T-202200/T^2)$	$1.265 \times 10^2(\exp(+168/T)$
621<T<744	$2.855 \times 10^{11} \times \exp(-15470/T)$	$2.157 \times 10^{10} \times \exp(-16070/T-207300/T^2)$	$6.602 \times 10^1(\exp(+48/T)$
T>744	$1.886 \times 10^8(\exp(-10150/T)$	$5.751 \times 10^8 \times \exp(-13530/T-136000/T^2)$	$9.971 \times 10^4(\exp(-4776/T)$

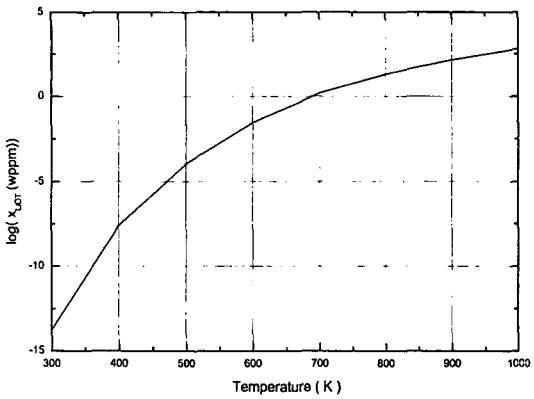

Fig. 1. Solubility Limit of LiOT in Li_2O

increases in logarithmic scale as the breeder temperature increases.

2.2. Kinetics of LiOT Formation and Decomposition

Tritium is produced in Li_2O grains by nuclear reactions and stabilized in the chemical status of LiOT [5]. This tritium diffuses to the grain surface where the following surface reactions take place. Tritium is released in various forms of gas phase species to the purge gas [12]. Among them T_2O or HTO are the most abundant and most influential on the overall tritium behavior [7, 13]. Therefore only two species are considered in this work. The decomposition rate constants for the LiOH(T) and LiOT according to the following reactions have been reported in [5,14]:

$$2\,LiOH(T) \Leftrightarrow Li_2O + H_2O(T_2O) \quad (2)$$

$$LiOT + LiOH(T) \Leftrightarrow Li_2O + HTO(T_2O) \quad (3)$$

For the first reaction the rate constant is given as:

$$k_d = 1.862 \times 10^8 \times \exp(-14920/T)\,[s^{-1}] \quad (4)$$

For the second reaction, the rate constant is given by:

$$k_d = 1.622 \times 10^7 \times \exp(-15520/T)\,[s^{-1}] \quad (5)$$

Using the equilibrium partial pressure of water over the two-phase system and the rate constant for decomposition, the rate constant for formation of LiOH (see Eq. (3)) can be obtained in the following way. At equilibrium we can write:

$$k_d\,[LiOT]^2 = k_f\,[Li_2O] \times [H_2O] \quad (6)$$

The equilibrium constant, K_{eq}, which equals k_d/k_f can be expressed in terms of the activities of the reactants and products as:

$$K_{eq} = a_{Li2O} \times P_{H2O} / (a_{LiOH})^2 \quad (7)$$

In the two-phase system the activities of both Li_2O and LiOH are equal to 1. Therefore:

$$K_{eq} = P_{H2O} = k_d/k_f \quad (8)$$

where P_{H2O} is the normalized pressure based on the atmosphere pressure.

Substituting for the partial pressure of water over the two-phase system shown in Table 1 and the decomposition rate constant, k_d, given by Eq. (5) into Eq. (8), the rate constant for formation of LiOH, k_f, can be obtained for various temperatures and also summarized in Table 1.

3. Description of the Developed Logic

The reported measured values of the LiOH(T) and Li_2O decomposition reaction rate constants are based on the rate of released moisture as the specimens are heated to certain temperatures. Therefore the derived values of the reaction rate constants, obtained in these experiments, in general, consist of the three processes: 1) tritium diffusion in the bulk; 2) LiOH(T) decomposition; and 3) surface recombination and desorption. The

kinetics of LiOH(T) formation will consist of the same three processes in reverse. The measured overall reaction rate constants, k_d (decomposition) and k_f (formation) can therefore be written in terms of the diffusion rate constant, k_{dif}, the bulk decomposition and formation rate constants, k_{db} and k_{fb}, and the surface desorption and adsorption rate constants, k_{des} and k_{ads} as:

$$1/k_d = 1/k_{db} + 1/k_{dif} + 1/k_{des} \quad (9)$$

$$1/k_f = 1/k_{fb} + 1/k_{dif} + 1/k_{ads} \quad (10)$$

The time constants for LiOT(H) formation and decomposition in the bulk, $1/k_{db}$ and $1/k_{fb}$, are for most cases much less than those of the diffusion and surface desorption. Therefore, for modeling of the kinetics of LiOT(H) formation and decomposition it is assumed that these processes are instantaneous. In other words, LiOH(T) precipitates instantaneously when the local tritium concentration exceeds the local tritium solubility limit in Li_2O and decomposes when the overall tritium concentration falls below the local solubility limit.

The governing equations used in MISTRAL code describing the diffusion and reactions of tritium are as follows:

$$\frac{\partial C_g}{\partial t} = D_g \nabla^2 C_g + G - \frac{\partial C_{LiOT}}{\partial t} \quad (11)$$

$$\frac{\partial C_{LiOT}}{\partial t} = k_f C_g - k_d C_s \quad (12)$$

where C_g [atms/m^3] is the tritium concentration in the grain, D_g [m^2/s] is the diffusion coefficient in the grain, G [atoms/m^3-s] is the uniform tritium generation rate in the grain and C_{LiOT} [atoms/m^3] is the LiOT concentration.

The following logic is added to the MISTRAL code to model the LiOT precipitation:

1) Find the solubility limit, C_{sl} for a local temperature using x_{LiOT} shown in Table 1. The unit of C_{sl} is atoms/m^3-s which is convertible to wppm by using a conversion factor.
2) Calculate the total tritium concentration, C_{tot}, in each location by adding the grain tritium concentration (C_g) obtained by solving the Eq. (11) and the LiOT concentration (C_{LiOT}) from the previous step:

$$C_{tot} = C_g + C_{LiOT} \quad (13)$$

3) Compare the total tritium concentration calculated in step 2) with the solubility limit calculated in step 1) and obtain the new concentrations of tritium in the grain and in LiOT, as follows:

$$\text{if } (C_{tot} > C_{sl}) \quad C_g = C_{sl},\ C_{LiOT} = C_{tot} - C_{sl} \quad (14)$$

$$\text{if } (C_{tot} < C_{sl}) \quad C_g = C_{tot},\ C_{LiOT} = 0 \quad (15)$$

4) March the time, $t = t + \Delta t$, with the newly defined concentration in step 2) and return.

4. Scenario for Verifying the Developed Logic

Preliminary calculations on the Li_2O-based solid breeder blankets indicated that no LiOT would precipitate due to the relatively high breeder temperatures and low tritium concentrations. On the other hand, no experimental data on the tritium release from Li_2O in the regime of LiOT formation is available yet. Therefore, to examine the effect of LiOT precipitation on the tritium release and inventory behavior in Li_2O, an arbitrary operation scenario is considered. Here the tritium generation rate remains at a constant value of G [atoms/m^3-s] and the breeder temperature follows the history consisting of a

600℃ plateau for 1000 s followed by 1000 s ramp-down to 100℃ and a 1000 s ramp-up to the original temperature of 600℃, as shown in Fig. 2. By repeating the calculations for values of generation rates in the range of 1×10^{18} - 1×10^{21} atoms/m^3-s with the same temperature history, the breeder temperature window in which LiOT forms as a function of tritium generation rate will be determined.

5. Results and Discussion

The given breeder temperature and tritium generation rate history were used as input to MISTRAL code to calculate the tritium release and inventory in Li_2O. Other input parameters used in this analysis are shown in Table 2. The results are shown in Fig. 2 and Fig. 3 in terms of tritium inventory (wppm) and normalized release fraction defined by the ratio of tritium release rate, R [atoms/m^3-s], to tritium generation rate, G [atoms/m^3-s], respectively. In Fig. 2, it is shown that during the initial high temperature period the tritium inventory as LiOT is zero and the grain (diffusive plus solubility) inventory is dominant. As the breeder temperature drops during the ramp-down, due to lower solubility, the grain inventory decreases and the surface inventory increases. At a temperature of about 340℃, LiOT begins to form and the tritium inventory as LiOT starts to increase as the temperature is further reduced. With the start of formation of LiOT both the grain and the surface inventories decrease. As the temperature increases during the ramp-up, tritium is still precipitated as LiOT up to a temperature of about 310℃. After that, the LiOT is decomposed and the tritium inventory as LiOT drops while the grain and surface inventories increase. At 380℃, all LiOT precipitate is decomposed. During the latter high temperature period of 600℃ grain inventory is dominant again. Fig. 2 clearly shows

Table 2. Input Parameters Used in the Tritium Transport Analysis

Li_2O Breeder Properties	
Sample Shape	Slab
Thickness, m	0.1
Sample Volume, m^3	4.872x10^{-6}
100% TD Density, kg/m^3	2000
Grain Radius, m	1.1x10^{-5}
Porosity, %	20
BET Area, m^2/kg	60
Helium Purge Gas	
Pressure, MPa	0.263
Flow Rate, m^3/s	1.667x10^{-6}
Hydrogen Concentration, %	0.1-0.01

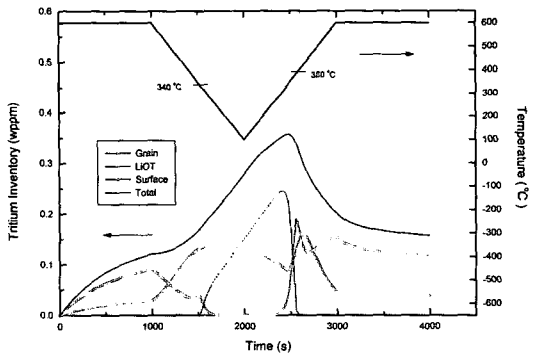

Fig. 2. Tritium Inventory Histories and Temperature Profile for G = 1×10^{20} atoms/m^3-s

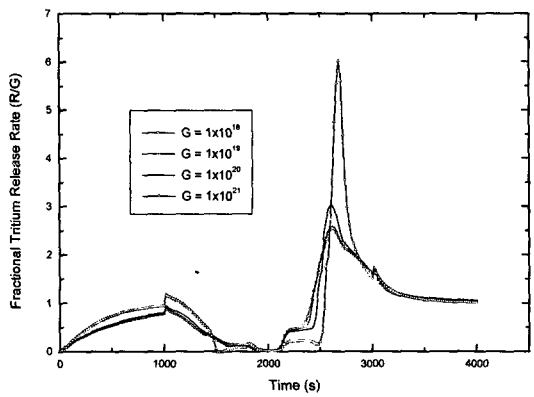

Fig. 3. Comparison of Normalized Tritium Release Fraction for Different Generation Rates

three temperature regimes. In the high temperature regime of 600℃, due to high solubility the grain inventory is dominant. In the intermediate temperature regime of about 350 - 600℃, the surface inventory becomes dominant. Finally, the inventory due to LiOT precipitation dominates over a temperature below about 350℃.

In Fig. 3 the normalized release fraction profile is shown along with the results for the different values of generation rates in the range of 1×10^{18} - 1×10^{21} atoms/m^3-s. The release rate increases and approaches to the steady state value of 1 during the initial constant temperature of 600℃. Since LiOT precipitation does not occur in this temperature regime, all amount of tritium generated in the grain release at steady state. When the temperature starts to decrease, a small peak appears due to instantaneous fast growth rate of surface inventory and decrease in grain inventory. During the ramp-down, the release rate decreases due to low grain inventory and slow surface reaction rate. As the temperature further decreases, tritium is trapped as LiOT and the release rate is very low and is almost zero below about 200℃. During the temperature ramp-up, LiOT precipitation disappears, and a substantial increase in the release rate is shown. This is due to instantaneous decomposition of LiOT and the high tritium inventory in the grain and surface. As shown in this figure, during the temperature regime of LiOT precipitation, flat tritium release rate is observed. In the early stage of the second high temperature region of 600℃, a small peak is shown as the fast decrease rate of surface inventory is slowed down. At the end of this temperature period, the tritium release rate approaches to the steady state value.

The normalized tritium release fraction profiles for the different generation rates are also shown in Fig. 3. As the tritium generation rate increases, similar profiles are shown, but higher peaks are

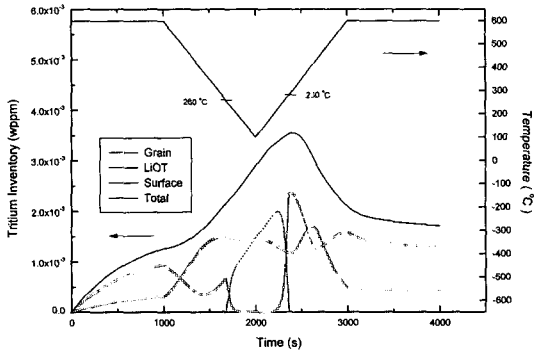

Fig. 4. Tritium Inventory Histories and Temperature Profile for G = 1×10^{18} atoms/m^3-s

shown. This is because the tritium inventory as LiOT becomes much greater as the tritium generation rate increases. In other words, higher LiOT precipitation, and higher instantaneous decomposition of LiOT occur with higher tritium generation rate, comparing the results shown in Fig. 4. The relative magnitude of the tritium inventory as LiOT is less than the grain inventory and similar to the surface inventory level as shown in Fig. 4. However, the relative magnitude of tritium inventory in LiOT is much greater than the other inventories, as shown in Fig. 2.

Comparing the results shown in Fig. 2 and Fig. 4, it is found that the temperature range of the tritium inventory as LiOT for G = 1×10^{20} atoms/m^3-s is wider and the peak of the inventory is higher than the results for G = 1×10^{18} atoms/m^3-s. It is also found that the overall inventory behaviors are similar for the different tritium generation rates. The temperature range for formation of LiOT, however, changes as the generation rate varies, such as 300 -320℃ for G = 1×10^{19} atoms/m^3-s, and 390 - 440℃ for G = 1×10^{21} atoms/m^3-s.

Fig. 5 shows the domain of breeder temperature and tritium generation rate over which LiOT precipitation is significant. The maximum and minimum limits appear due to non-symmetry concentration profile in the grain. Therefore,

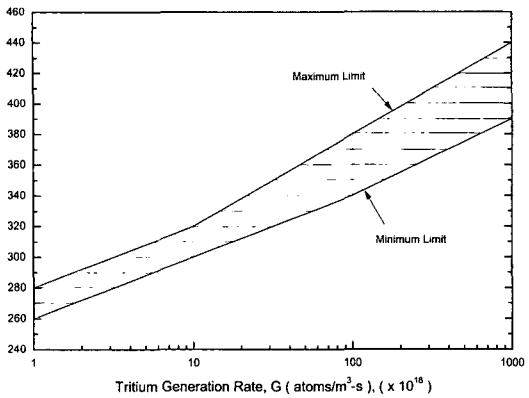

Fig. 5. Region of LiOT Precipitation in Li_2O Ceramics

LiOT precipitation is an important tritium transport mechanism in Li_2O solid breeder under any pulsed operation of the hatched region. It may be noted that tritium chemistry is sensitive to the hydrogen amounts in the purge gas. However, similar results can be obtained with the hydrogen concentration ranges shown in Table 2.

6. Conclusions

Based on the available thermodynamics and kinetics data, a logic for predicting LiOT formation and decomposition in Li_2O solid breeder was developed and integrated in the MISTRAL computer code. This logic is based on the comparison of the local tritium concentration and tritium solubility in Li_2O and defines the tritium concentration in the grain and as LiOT. With this logic the code is capable of predicting tritium inventory as LiOT precipitate under steady state and transient operating conditions. Using a transient temperature scenario and the tritium generation rates in the range of 1×10^{18} - 1×10^{21} atoms/m^3-s, the temperature limits for the formation and decomposition of LiOT and the temperature regimes were determined. Here, each of the three forms of tritium inventory (grain, surface and precipitation) is dominant for different tritium generation rates. Therefore the code integrated with the developed logic is useful for the transient analysis of the tritium transport in fusion blanket material under pulsed environment.

References

1. K. Ioki et al., "Design and Material Selection for ITER First Wall/Blanket, Divertor and Vacuum Vessel," J. of Nuclear Materials, Vol. 258-263, pp. 74-84 (1998).
2. C.E. Johnson, "Research and Development Status of Ceramic Breeder Materials," J. of Nuclear Materials, Vol. 179-181, pp. 42-56 (1991).
3. N. Roux, C. Johnson and K. Noda, "Properties and Performance of Tritium Breeding Ceramics," J. of Nuclear Materials, Vol. 191-194, pp. 15-22 (1992).
4. N. Roux et al., "Summary of Experimental Results for Ceramic Breeder Materials," Fusion Engineering and Design, Vol. 27, pp. 154-166 (1995).
5. H. Moriyama, S. Tanaka and K. Noda, "Irradiation Effects in Ceramic Breeder Materials," J. of Nuclear Materials, Vol. 258-263, pp. 587-594 (1998).
6. G. Federici, A.R. Raffray and M.A. Abdou, "MISTRAL: A Comprehensive Model for Tritium Transport in Lithium Base Ceramics-Part I and II," J. of Nuclear Materials, Vol. 173, pp. 184-228 (1990).
7. A. Badawi, Modeling and Analysis of Time-Dependent Tritium Transport in Lithium-Containing Ceramics, Ph.D. Dissertation, University of California, Los Angeles, (1993).
8. M. Tetenbaum, A.K. Fisher and C.E. Johnson, "An Investigation of the Solubility of LiOH in Solid Li_2O," Fusion Technology, Vol. 7, pp. 53-56 (1985).

9. M. Tetenbaum, and C.E. Johnson, "Partial Pressures of H_2O above the Diphasic Li_2O-LiOH(s,l) System," J. of Nuclear Materials, Vol. 126, pp. 25-29 (1984).
10. H. Takeshita and H. Watanabe, "Equilibrium Pressures of H_2O(g) over the Li_2O(s)-LiOH(s) System," J. of Nuclear Materials, Vol. 207, pp. 92-97 (1993).
11. N.W. Gregory and R.H. Mohr, "The Equilibrium 2 LiOH(s) + H_2O(g)," J. Am. Chem. Soc., Vol. 77, pp. 2142 (1955).
12. A.K. Fisher and C.E. Johnson, "Thermodynamics of Li_2O Fusion Reactor Breeder," J. of Nuclear Materials, Vol. 126, pp. 268-275 (1984).
13. A. Badawi, A.R. Raffray, A. Ying and M.A. Abdou, "Tritium Analysis for the US-ITER Solid Breeder Blanket," Fusion Technology, Vol. 19, pp. 1532-1537 (1991).
14. H. Kudo, "The Rate of Thermal Decomposition of LiOH(s), LiOD(s) and LiOT(s)," J. of Nuclear Materials, Vol. 87, pp. 185-188 (1979).